International Journal of Mechanical Engineering (IJME)
ISSN(P): 2319-2240; ISSN(E): 2319-2259
Vol. 5, Issue 1, Dec –Jan 2015, 15-26

International Academy of Science, Engineering and Technology
Connecting Researchers; Nurturing Innovations

INFLUENCE OF SPECIMEN GEOMETRY AND LUBRICATION CONDITIONS ON THE COMPRESSIONBEHAVIOR OF AA6066 ALUMINUM ALLOY

OSAMA MOHAMED IRFAN

Department of Mechanical Engineering, Faculty of Engineering,

Qassim University, KSA, BaniSuief University, Egypt

ABSTRACT

In this work, the results from a series of experiments are presented to determine the effect of specimen geometry/dimensions on the compression behavior of AA6066Al alloy. Three geometries of compression specimens have been used; solid, tapered and collar. For each geometry, the compression tests have been carried out under dry and lubricated conditions. The experiments have been conducted at various aspect ratios: H_o/D_o; 1.5, 1.25, 1, 0.75, and 0.5. The results showed that the circumferential strain ε_θ of the cylindrical specimens increases as the axial strain ε_z increases. For collar specimens, the values of local strain ε_z are inversely proportional to the total axial strain, while for tapered specimens, the local circumferential strains ε_θ are very close to the total circumferential strain.

KEYWORDS: Specimen Geometry, Compression Test, True Stress-Strain, AA6066Al Alloy

INTRODUCTION

Aluminum alloys and composites have been the material of choice for aerospace, automotive, and military applications. Al-6xxx alloys have various benefits including medium strength, formability, weldability, corrosion resistance, and low cost [1]. Hence, mechanical characterization of the alloy and processing procedure are important for that approach. Compression behavior of Al-6xxx alloys has been the subject of many studies[2 and 3].Compression testing has become increasingly popular for several reasons; in particular (a) Uniform deformation can be achieved for large strains with proper lubrication. (b) The compressive state closely represents the conditions present in various forming processes such as forging, extrusion and rolling. Among the various types of hot compression tests, the constant strain rate test is preferred[4-6].There is a great interest in the compression process due to the industrial demands to produce light weight and high strength components. The large number of parameters involved in forming by compression makes the process more complex. These topics were studied previously in many researches with different viewpoints. The examined parameters include material properties, machine parameters, work piece geometry and working conditions [7-11]. However, several types of plastic instabilities can be developed in the compression tests. The first type is associated with a maximum in the true stress- true strain curve. The second type concerns inhomogeneous deformation and shear band. At certain strain rates and temperatures some strengthening mechanisms become unstable [12].The axial true strain ε_z and circumferential true strain ε_θ on barreled surface of the circular compression specimen that illustrated by the model shown in Figure 1 can be calculated by using the relations given in Eq.1 and 2.

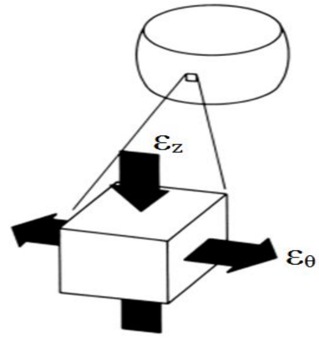

Figure 1: Localized Strains on the Bulging Cylindrical Surface of a Compression Test Specimen

For axial true strain,

$\varepsilon_z = \ln (H_f/H_o)$ (1)

For circumferential true strain,

$\varepsilon_\theta = \ln (D_f/D_o)$ (2)

Where H_o and H_f are initial and final gauge heights, respectively; D_o and D_f are initial and final diameters, respectively.

Stresses at the free surfaces of compressed specimens can be calculated by using Levy-Mises equations as follows[12]:

$d\varepsilon_r = d\lambda[\sigma_r - (\sigma_\theta + \sigma_z)/2]$ (3)

$d\varepsilon_\theta = d\lambda[\sigma_\theta - (\sigma_r + \sigma_z)/2]$ (4)

$d\varepsilon_z = d\lambda[\sigma_z - (\sigma_\theta + \sigma_r)/2]$ (5)

The equivalent strain $d\varepsilon$, and equivalent stress σ are obtained by:

$$d\varepsilon = \frac{\sqrt{2}}{3}[(d\varepsilon_r - d\varepsilon_z)^2 + (d\varepsilon_z - d\varepsilon_\theta) + (d\varepsilon_\theta - d\varepsilon_r)^2]^{1/2} \quad (6)$$

$$\sigma = \frac{1}{\sqrt{2}}[(\sigma_r - \sigma_z)^2 + (\sigma_z - \sigma_\theta)^2 + (\sigma_\theta - \sigma_r)^2]^{1/2} \quad (7)$$

Where $d\varepsilon_r$, $d\varepsilon_\theta$, and $d\varepsilon_z$ are the strain components in r, θ, and z directions; σ_r, σ_θ, and σ_z are the stress components$r$, θ, and z directions; and $d\lambda$ is proportionality constant that depend on material and strain level.

Uniaxial compression testing is still the dominant means for characterizing the mechanical behavior of metals and alloys. Disparities in testing procedures and methodologies are clearly observed among the various efforts in the literature, often leading to differences in the collected data, even when investigating the same material.The ASTM E9-09and the ASTM E209-00 are the two major standards for testing materials in compression[13 and14]. Sometimes the standards neither agree on several testing aspects nor offer any reasoning to how the suggested testingparameters were selected, especially the dimensions and proportions of the test specimen. Whether it is due to their recent publication, the lack of generality, or their apparent disagreements; the standards has not had a great impact, and most efforts on characterizing the mechanical behaviors of materials are still scattered. Examples of recent efforts in the field show that the investigators utilized test specimens with different dimensions[15-17]. It is probably tolerable to suppose that the size of a compression test specimen is not greatly influential to the obtained stresses and strains. Measured forces and displacements, from which the latter are derived, are correlated to the initial size of the specimens gauge section. This could be a major source of errors in the obtained stress-strain behavior [18 and19], hence indicating the need to optimize the proportions of the specimen geometry. Ivanisevic Ajose et al. [20] performed an experimental study on formability of brass by applying compression tests. The obtained experimental data was used in designing and forming the limit diagram. It has been reported that specimen geometry as well as loading mode affects strength characteristics in metals, alloys and composites [21-32].The effective volume proposed by Davies [33] has been applied to evaluate the effect of specimen geometry on strength in ceramics [34]. Lowhaphandu et al. [35and 36] examined mechanical properties of Zr–Ti–Ni–Cu–Be by using different dimensions of specimens and they found great differences. T. Klunsner et al. [37] studied the effect of specimen size on the strength of WC–Co hard metal. The results showed that the determined fracture strength values vary significantly with specimen size. D.J. Smith et al. [38] conducted a series of experiments to determine the effect of specimen dimensions on the ductile resistance of A508 Class3 forged steel at ambient temperature. The results showed a decrease in the slope of the tearing resistance with increasing specimen size.

The present work attempts to shed light on the mechanical behavior of AA6066 Al alloy depending on specimen geometry under uniaxial compression loading conditions. Three types of specimens: solid, tapered, and collar were produced. The compression tests under dry and lubrication conditions were conducted at various aspect ratios (H_o/D_o).

Experimental Work

Material

The investigations were carried out on AA6066 Aluminum alloy, as-received material with the chemical composition stated in Table 1.

Table 1: Chemical composition of the AA6066 Aluminum Alloy (wt.%)

Component	Si	Mg	Cu	Mn	Fe	Cr	Al
Wt. %	0.9	0.8	0.7	0.6	0.5	0.4	Balance

Specimen Preparation and Test Procedure

Six upset sample geometries were designed and machined. The samples are identified as SU (short upset, no lubricant), SUL (short upset, lubricant), LU (long upset, no lubricant), LUL (long upset, lubricant), CU (collar upset, no lubricant), and CUL (collar upset, lubricant). The initial dimensions and drawings of the specimens are presented in table 2. The specimens of AA 6066 Alalloy with the required dimensions were prepared by machining process and cut by using a precision cut off machine running at low speed. The machined specimens were polished with fine sandpaper to remove any machining marks from the surface

Table 2: Initial Dimensions of Specimens Used in Experiments

Specimen Type	Lubrication Conditions	Original Dimensions, (mm)		Aspect Ratio, H_o/D_o	Drawing
		Height, H_o	Diameter, D_o		
Solid (Basic cylinder billet)	Dry/Lubricated	37.5	25	1.5	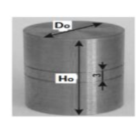
		31.25	25	1.25	
		25	25	1	
		18.75	25	0.75	
		12.5	25	0.5	

Tapered test billets	Dry/Lubricated	37.5	25	1.5	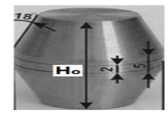
		31.25	25	1.25	
		25	25	1	
		18.75	25	0.75	
		12.5	25	0.5	
Collar cylinder test billet	Dry/Lubricated	37.5	25	1.5	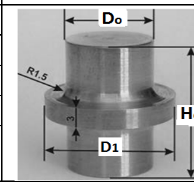
		31.25	25	1.25	
		25	25	1	
		18.75	25	0.75	
		12.5	25	0.5	

In order to perform the compression tests under lubricated conditions, friction conditions were reduced by applying graphite based lubricant to the contact surfaces. For solid and tapered specimens, a portion of the surface was machined with circumferential grids. All compression tests were carried out by using servo hydraulic testing machine, model 4505 with a capacity of 200 ton. The tests weredone under displacement control at a constant rate of approximately 0.5 mm/min. In each case, applied load and axial displacement were measured and recorded.

RESULTS AND DISCUSSIONS

Deformation Ratio

The maximum deformation ratios (H_f/H_o)of AA6066Al alloy with various specimens geometries and aspect ratios are shown in Figures 2-4. It can be observed from Figure 2 (a) that H_f/H_o ratios for solid specimens are higher in case of lubricated specimens than for dry ones. The highest deformation ratio for non-lubricated solid specimens was 49% while for lubricated specimens it was 51%. Those values recorded at an aspect ratio H_o/D_o of 1. The lowest deformation ratios was 31% and 42% for dry and lubricated specimens respectively, this occurred at an as pectratio H_o/D_o of 1.25. Figure 2 (b) shows specimens after compression test and it is noticed the cracks on the lateral free surface of the specimens that imposed to non-lubricated conditions rather than the lubricated specimen.

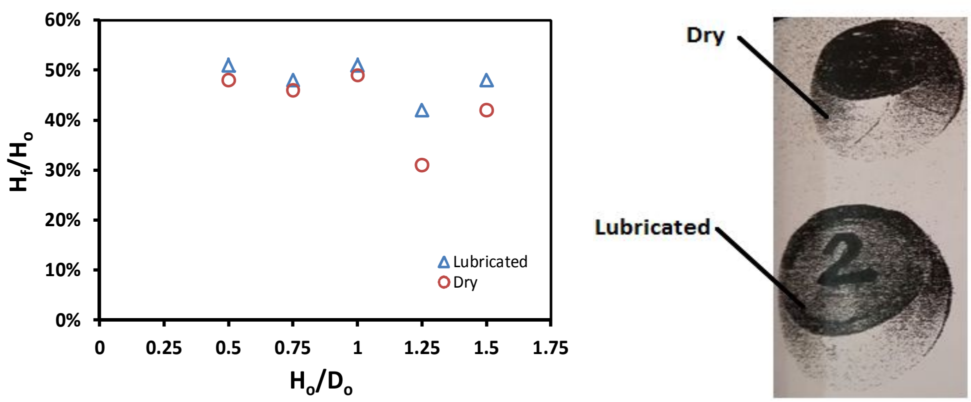

(a) (b)

Figure 2: (A) Deformation Ratio of Solid Specimens at Various Aspect Ratios H_o/D_o(B) Solid Specimens after Compression Test

Figure 3 (a) shows the deformationratio (H_f/H_o) of tapered specimens. The greatest H_f/H_o ratio for lubricated specimens was 67% at H_o/D_o=1, while for non-lubricated condition the greatest H_f/H_o ratiowas 52% corresponding to H_o/D_o of 0.5. The compressed specimens with clear cracks for both dry and lubricated conditions are shown in Figure 3 (b).

The compression ratio (H_f/H_o) of tapered specimens at various ratios of H_o/D_o is illustrated in Figure 4 (a). It can be seen that the greatest H_f/H_o ratio for lubricated specimens was 72% that corresponding to H_o/D_o of 0.75. For non-lubricated specimens the maximum H_f/H_o was 74% corresponding to H_o/D_o of 1.5.

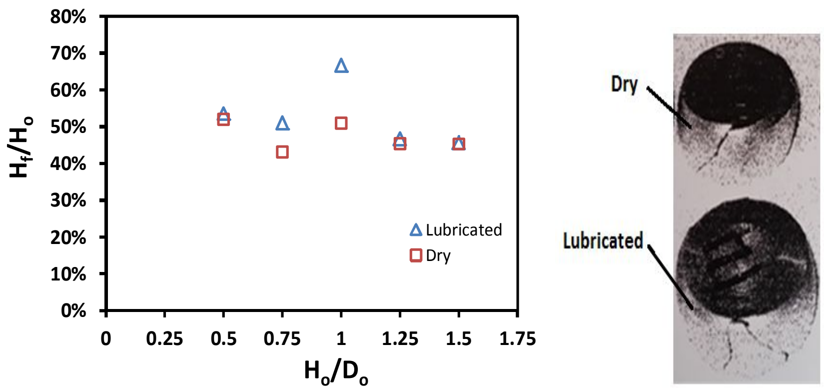

(a) (b)

Figure 3: (A) Deformation Ratio of Tapered Specimens at Various aspect Ratios H_o/D_o (B) Tapered Specimens after Compression Test

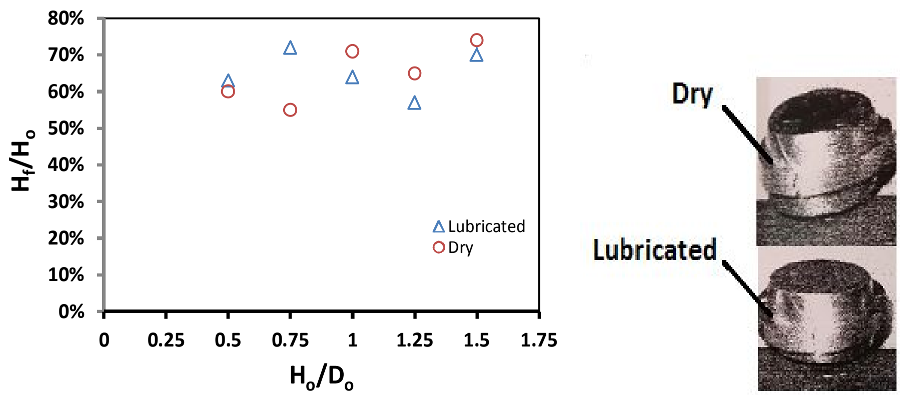

(a) (b)

Figure 4: (a) Deformation Ratio of Collar Specimens at Various aspect Ratios H_o/D_o (b) Collar Specimens after Compression Test

True Stress–Strain Behavior for Solid Non-Lubricated Specimens

The true stress–strain curves of the AA6066 Al alloy for solid non- lubricated specimens suffered the compression deformation are shown in Figure 5. Obviously, the effects of aspect ratio on the true stress- true strain are significant for all the tested conditions. As can be seen from the results, there is a systematic trend toward the increase in true stress with increasing true strain for all aspect ratios[39]. The true stress–strain curves exhibit a maximum stress values at an aspect ratio H_o/D_o of 0.75, while minimum stresses were observed at H_o/D_o ratio of 1.25.

True Stress–Strain Behavior for Solid Lubricated Specimens

The effect of aspect ratio H_o/D_o on the true stress- strain of AA6066 Al alloy for solid lubricated specimens is shown in Figure 5. It can be observed that, the true stress–true strain curves exhibit a maximum stress values at an aspect ratio of 1, while minimum stresses occurred at a ratio of 1.25.

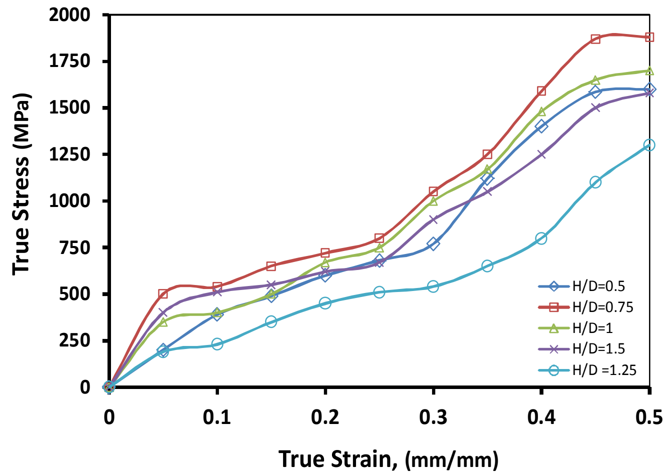

Figure 5: True Stress–Strain for Solid Non-Lubricated Condition

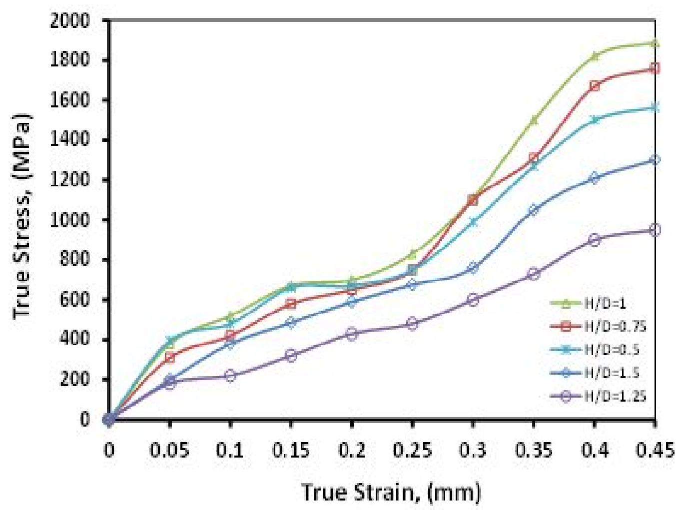

Figure 6: True Stress–Strain for Solid Lubricated Specimens

True Stress–Strain Behavior for Tapered Non-Lubricated Specimens

Figure 7 shows the effects of aspect ratio H_o/D_o on the true stress- strain of AA6066 Al alloy for tapered non-lubricated conditions. It is shown that, at low strains (0 - 0.2) the true stress curves exhibit a maximum stress when H_o/D_owas1.5, while at higher strains (0.25 - 0.4) the maximum stress occurred when the value of H_o/D_o was 0.75. For the all values of strain, the lowest stresses occurred at H_o/D_o ratio of 0.5.

True Stress–Strain Behavior for Tapered Lubricated Specimens

The effect of aspect ratio H_o/D_o on the true stress- strain of AA6066 Al alloy for tapered lubricated specimens is illustrated in Figure 8. The graph shows maximum stresses at H_o/D_o of 1.5, while minimum stress occurred at a ratio of 0.5.

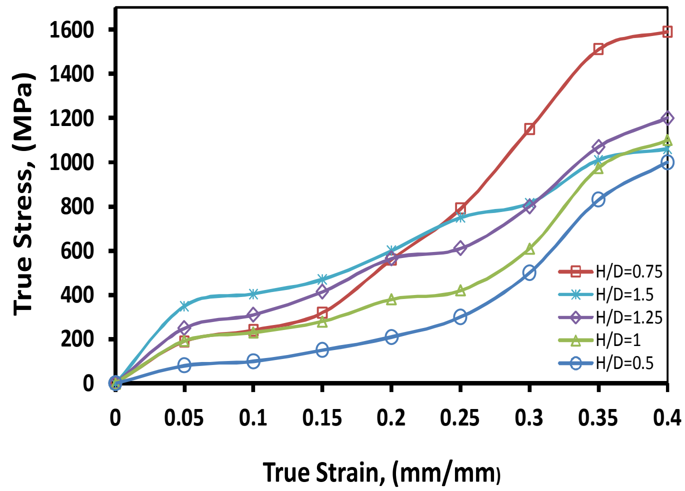

Figure 7: True Stress–Strain for Tapered Non- Lubricated Specimens

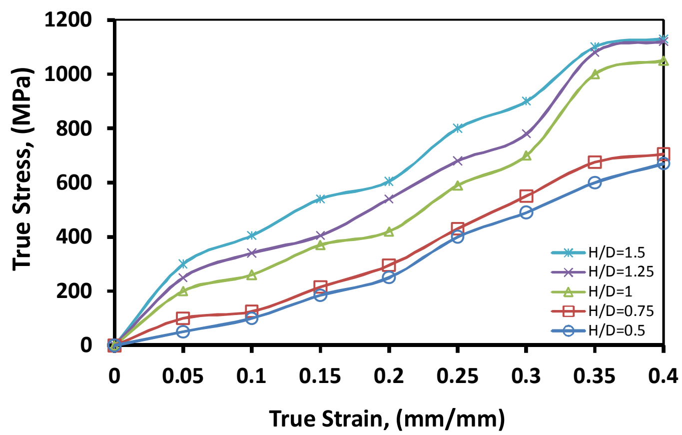

Figure 8: True Stress–Strain for Tapered Lubricated Specimens

True Stress–Strain Behavior for Collar Non-Lubricated Specimens

Figure 9 shows the effect of aspect ratio H_o/D_oon the true stress- strain of AA6066 Al alloy for collar non- lubricated specimens. It is shown that, the true stress–true strain curves have maximum stresses at H_o/D_o of 0.75, while minimum stress occurred at a ratio of 0.5.

True Stress–Strain Behavior for Collar Lubricated Specimens

Figure 10 shows the effect of aspect ratio H_o/D_o on the true stress- true strain of AA6066 Al alloy for collar lubricated specimens. It is shown that, the true stress–strain curves have maximum stresses at a H_o/D_o of 0.75, while minimum stress occurred at a ratio of 0.5.

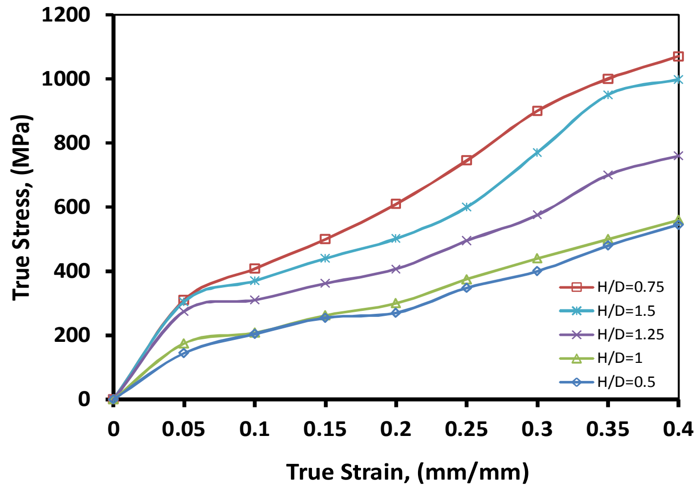

Figure 9: True Stress–Strain for Collar Non-Lubricated Specimens

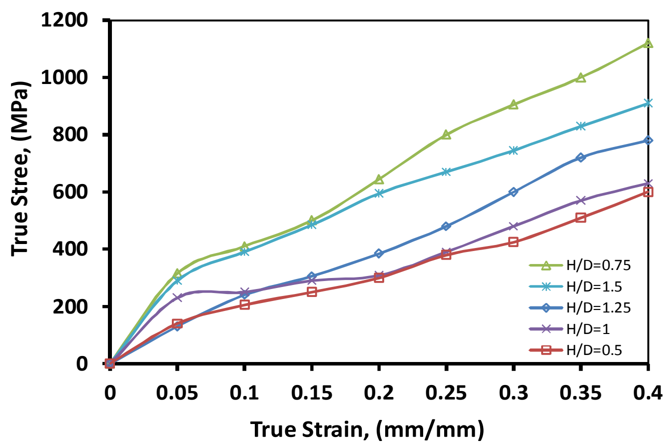

Figure 10: True Stress–Strain for Collar Lubricated Specimens

The interpretation of true stress-strain behavior after the compression tests can be stated as follows: in case of tapered and collar compression test specimens the interior deformation of the cylinder expands the central region, accentuating the circumferential tension. Because the free surface at midheight is not directly in contact with the platen surface along straight line, compression of this section is less than in cylindrical compression [40]. At the free surfaces of compressed cylinders, the strain consists of circumferential tension and axial compression.

CONCLUSIONS

The effect of specimen geometry/dimensions on deformation ratio and behavior of true stress-strain forAA6066 Al alloy have been investigated. For all tested geometries, the true stress increases with increasing the aspect ratio H_o/D_o of the specimen. Regarding the cylindrical solid specimens, the value of circumferential strain ε_θ increases as the axial strain ε_z increases. The values of local strains are proportional to the total strains. For collar specimens, the values of local strain ε_z are inversely proportional to the total axial strain, while for tapered specimens, the local circumferential strains ε_θ are very close to the total circumferential strain

REFERENCES

1. E. Tan and B. Ogel, “Influence of Heat Treatment on the Mechanical Properties AA6066 Alloy,” Turkish Journal of Engineering and Environmental Sciences, Vol. 31, (2007), pp 53-60.
2. Waldemar A. Monteiro, Iara M. Esposito1, Ricardo B. Ferrari, Sidnei J. Buso, microstructural and Mechanical Characterization after Thermomechanical Treatments in 6063 Aluminum Alloy”, Materials Sciences and Applications, (2011), 2, 1529-1541
3. A.F. Manzellaa, B.A. Gamab, and J.W. Gillespie Jr.” Effect of punch and specimen dimensions on the confined compression behavior of S-2 glass/epoxy composites”, Composite Structures, Volume 93, Issue 7, (2011), p.p. 1726–1737
4. Narayanamurthy. S.V, Nageswararao. B and Kashyap. B.P, “Instability Criteria for Hot Deformation Behaviour of Materials”, *International Materials Review*, (2000), vol.45, No.1, pp15-26.
5. Cho.J.R, Bae.W.B, Hwang.W.J, and Hartely.P, “A Study on Hot Deformation Behavior and Dynamic Recrystallization of Al-5 Wt.% Mg Alloy”, *Journal of Material Processing Technology*, (2001), vol.118, pp 356-361.
6. Gourdet.S and Montheillet. F, “An Experimental Study of the Recrystallization Mechanism during Hot Deformation of Aluminium”, *Material Science and Engineering A*, (2000), vol.283, pp274-288.
7. Mustafa Yasar, Halil Ibrahim Demirci, Ibrahim Kadi, “Detonation forming of aluminum cylindrical cups experimental and theoretical modelling” Journal of Materials & Design, Elsevier Publications, 27, (2006) 397-404.
8. Y. X. Tian, G. Wang, S. Yu, and Z. T. Yu,” Microstructure characteristics and strain rate sensitivity of a biomedical Ti–25Nb–3Zr–3Mo–2Sn titanium alloy during thermomechanical processing”, J Mater Sci (2015) 50:5165–5173
9. Ganesh M. Kakandikar and Vilas M. Nandedkar, “Some Studies on Forming Optimization with Genetic Algorithm”, An International Journal of Optimization and Control: Theories & Applications Vol.2, No.2, (2012) pp.105-112.
10. Mustafa Yasar, ZekiKorkmaz, MuammerGavas “Forming sheet metals by means of multi-point deep drawing method” Journal of Materials & Design, Elsevier Publications, 28, (2007) 2647-2650.
11. ErkanOnder, A. ErmanTekkaya “Numerical simulation of various cross sectional work pieces using conventional deep drawing and hydro forming technologies” Journal of Machine Tool & Manufacture, Elsevier Publications, 48, (2008) 532- 535.
12. G.E. Dieter, H.A. Kuhn, and S.L. Semiatin, “ Handbook of workability and process design”, ASM International, (2003), p.p. 57-66
13. “Standard Test Methods of Compression Testing of Metallic Materials at Room Temperature”, ASTM E9-09, (2009).

14. "Standard Practice for Compression Tests of Metallic Materials at Elevated Temperatures with Conventional or Rapid Heating Rates and Strain Rates", ASTM E209-00, (2010).
15. P. Mukhopadhyay, S. Biswas, and A. Chokchi, Deformation Characterizationof Superplastic AA7475 Alloy, Trans. Indian Inst. Met., (2009), 62(2), p.p. 149–152.
16. F. Abu-Farha and M. Khraisheh, Analysis of Superplastic Deformation of AZ31 Magnesium Alloy, J. Adv. Eng. Mater., (2007), 9(9), p 777–783
17. J. Chang, E. Taleff, and P. Krajewsky, Effect of Microstructure onCavitation during Hot Deformation of a Fine-Grained Aluminum- Magnesium Alloy as Revealed through Three-Dimensional Characterization, Metall. Mater. Trans. A,, 40(13), (2009) p.p. 3128–3137.
18. K. Johnson, M. Khaleel, C. Lavender, S. Pitman, J. Smith, M. Smith, and C. Hamilton, The Effect of Specimen Geometry on the Accuracy of Constitutive Relations in a Superplastic 5083 Aluminum Alloy, Mater. Sci. Forum, (1994), 170–172, p.p. 627–632.
19. Emad Abdelraouf BADAWI*, Mmdouh ABDEL-NASER and AlaaAldeen AHMED, "Influence of Plastic Deformation on the Properties of 6066 HeatTreatable Aluminum Alloys", Waiaiiak J Sei& Tech (2013); 10(3): 289-295.
20. Ivanisevic Aljosa, ViloticDragisa, Kacmarcik Igor, MilutinovicMladomir," Upsetting of brass billets by flat dies", Journal for Technology of Plasticity, v. 38 (2013), No. 2.
21. Jones, R. L. and Rowclike, D. J. Tensile-strength distribution for silicon nitride and silicon carbide ceramics. Ceramics Bulletin, (1979), 58, 836-839.
22. Shetty, D. K., Rosenfield, A. R., Bansal G., K. and Duckworth, W. H. Biaxial fracture studies of a glass-ceramic. Journal of the American Ceramic Society, (1981), 64, 1-4.
23. Bansal, G. K., Duckworth, W. H. and Niesz, D. E. Strength-size relations in ceramic materials: Investigation of an alumina ceramic. Journal of the American Ceramic Society, (1982), 59, 472-478.
24. Katayama, Y. and Hattori, Y. Effects of specimen size on strength of sintered silicon nitride. Journal of the American Ceramic Society, (1982), 65, C164-C165.
25. Matsusue, K., Takahara, K. and Hashimoto, R. Strength evaluation test of hot-pressed silicon nitride at room temperature. Yogyo-Kyokai-Shi, (1982), 90, 168-174.
26. Matsusue, K., Takahara, K. and Hashimoto, R. Strength evaluation of pressureless-sintered SiC and reaction-sintered Si3N4 at room temperature. Yogyo-Shi, (1982), 90, 280-282.
27. Neal, D. M.Lenoe, E. M. Examination of size effects in the failure prediction of ceramic material. Fracture Mechanics of Ceramics, ed. Bradt et al. Plenum Press, New York, (1983), 5, 387-401.
28. Fessler, H., Fricker, D. C. and Godfrey, D. J. A comparative study of the mechanical strength of reaction-bonded silicon nitride. Ceramics-Performance Applications, (1983), 3, 705-736.

29. Shetty, D. K., Rosenfeld, A. R. and Duckworth, W. H. Statistical analysis of size and stress state effects on the strength of an alumina ceramic. ASTM STP, (1984), 844, 57-80.
30. Yamada, T. and Hoshide, T., Reliability of ceramic materials for static and cyclic loads. In Proceedings of ICOSSAR 85 II. International Association for Structural and Reliability,Columbia University, New York, 1985, pp. 441-450.
31. Soma, T., Matsui, M. and Oda, I., Tensile strength of a sintered silicon nitride. In Non-Oxide Technical and Engineering Ceramics, ed. Hampshire, S. Elsevier, Oxford, (1986), pp. 361-374.
32. Kschinka, B. A., Perrella, S., Nguyen, H. and Bradt, R. C. Strength of glass spheres in compression. Journal of the American Ceramic Society, (1986), 69, 467-472.
33. [33] Davies, D. G. S., The statistical approach to engineering design in ceramics. In Proceedings of the British Ceramic Society 22. (1973), pp. 429-452.
34. Toshihiko Hoshide, Jun Murano and RyosukeKusaba, “Effect of specimen geometry on strength in engineering ceramics”, Engineering Fracture Mechanics Vol. 59, No.5, (1998), pp. 655-665.
35. P Lowhaphandu, L.A Ludrosky, S.L Montgomery, and J.J Lewandowski, “Deformation and fracture toughness of a bulk amorphous Zr–Ti–Ni–Cu–Be alloy”, Intermetallic, v. 8, No.5–6, (2000), p.p. 487–492.
36. F.X. Liua, P.K. Liawa, G.Y. Wanga, C.L. Chianga, b, D.A. Smitha, P.D. Racka, J.P. Chub, and R.A. Buchanana, “Specimen-geometry effects on mechanical behavior of metallic glasses”, Intermetallics, v. 14, No. 8–9, (2006), p.p. 1014–1018.
37. T. Klünsner, S. Wurster, P. Supancic, R. Ebner, M. Jenko, J. Glätzlee, A. Püschele,and R. Pippan, “Effect of specimen size on the tensile strength of WC–Co hard metal”, ActaMaterialia, v. 59, No. 10, (2011), p.p. 4244–4252.
38. D.J. Smith, T.D. Swankie, M.J. Pavier, M.C. Smith, “The effect of specimen dimensions on mixed mode ductile fracture”, Engineering Fracture Mechanics, 75 (2008) 4394–4409
39. Gourdet S, Montheillet F An experimental study of the recrystallization mechanism during hot deformation of aluminium. Mater SciEng A 283(1–2): (2000) 274–288
40. H.P. Ganser, A.G. Atkins, O. Kolednik, F.D. Fischer, and O. Richard,” Upsetting of cylinders: A comparison of two different damage indicators”, J. Eng. Mater. Techol.,v.123, (2002), p.p.94-99.